

Microscopic Analysis of the Low-Lying Even Parity Bands in ^{168}Er

Huang Haixin, Wu Chongshi and Zeng Jinyan

(Department of Physics, Beijing University, Beijing)

Taking into account the pairing plus quadrupole-quadrupole interaction, the intrinsic properties of the low-lying bands (even parity) and the related $E2$ transition probabilities in ^{168}Er were calculated in the frame of Bohr-Mottelson-Nilsson model. The agreement between the calculated and the observed results is satisfactory. Some difficulties encountered in the IBM prediction do not appear in the present calculation.

1. INTRODUCTION

Recently comprehensive experimental studies[1--5] of the well-deformed nucleus ^{168}Er have provided the most detailed and complete level scheme for an even-even deformed nucleus. The observed overall level scheme, including more than 20 rotational bands, is believed to be complete for all levels with $I \leq 6$ and $E_x \lesssim 2$ MeV. These valuable data offer an ideal opportunity to test the various nuclear models.

In Ref.[6] the positive parity bands of ^{168}Er were investigated by Warner et al. in the frame of interacting boson model (IBM, only the s and d bosons included). The main achievements are as follows: the observed three $K^\pi = 0^+$ excited bands and three $K^\pi = 2^+$ excited bands can be reproduced; the calculation provided a good description to some of the $E2$ transition properties, especially the dominance of the $E2$ transitions from the 0_2^+ band (β -band) to the 2_1^+ band (γ -band) over those to the ground band. However, Bohr and Mottelson[7] pointed out that there still exist serious disagreements between the IBM prediction and the experiment. The following points are noteworthy:

(1) The IBM predicts a $K^\pi = 4_1^+$ band at 1619 keV, whereas the two observed lowest-lying $K^\pi = 4^+$ bands locate above 2 MeV, which reveals a strong anharmonicity in the γ -vibrational mode. In addition, the 2_3^+ band is predicted at too high energy.

(2) The observed $E2$ transition probabilities from the 0_3^+ band to the ground band are significantly (two order of magnitude) stronger than those predicted by the IBM.

(3) The observed $K^\pi = 3^+$ band at 1653 keV cannot be reproduced in the sd -IBM description. Though the incorporation of g bosons may account for the above discrepancy[8], the number of parameters increases.

(4) To account for the numerous observed negative parity bands, f -boson must be involved. However, according to the experimental results and analysis of Burke et al.[4,5], some negative parity bands, e.g. the 4_1^- and 1_1^- bands, show a two-quasiparticle character and are hard to be brought into the frame of IBM description.

In the present paper, the nuclear pairing correlation and the long range quadrupole-quadrupole interaction are taken into account in the frame of the Bohr-Mottelson-Nilsson model to analyze the intrinsic properties of the low-lying excitation bands (even parity) in ^{168}Er and the related $E2$ transition probabilities.

2. CALCULATION

In the Bohr-Mottelson-Nilsson frame, the intrinsic Hamiltonian which includes the pairing plus quadrupole-quadrupole interactions is expressed as follows[9]:

$$H_{\text{intr}} = H_{\text{sp}} + H_{\text{p}} + H_{\text{Q}}, \quad (1)$$

where H_{sp} is the Nilsson single particle Hamiltonian[10] (the deformation parameters are taken from the Lund systematics[11]), H_{p} is the pairing interaction and H_{Q} the quadrupole-quadrupole interaction.

In the representation in which H_{sp} is diagonal, H_{p} is expressed as:

$$H_{\text{p}} = \sum_{\mu > 0} \epsilon_{\mu}^{\text{p}} (a_{\mu}^{\dagger} a_{\mu} + a_{\bar{\mu}}^{\dagger} a_{\bar{\mu}}) + \sum_{\nu > 0} \epsilon_{\nu}^{\text{n}} (b_{\nu}^{\dagger} b_{\nu} + b_{\bar{\nu}}^{\dagger} b_{\bar{\nu}}), \quad (2)$$

where μ, ν label the Nilsson single particle states, and $\bar{\mu}, \bar{\nu}$ are their time reversal states, respectively. $\epsilon_{\mu}^{\text{p}}$ and $\epsilon_{\nu}^{\text{n}}$ are the proton and neutron Nilsson energy levels (twofold degenerate), respectively. $a^{\dagger}(a)$ and $b^{\dagger}(b)$ are proton and neutron creation (annihilation) operators, respectively. The pairing interaction is expressed as:

$$H_{\text{p}} = -G_{\text{p}} \sum_{\mu, \mu' > 0} a_{\mu}^{\dagger} a_{\bar{\mu}}^{\dagger} a_{\mu'} a_{\bar{\mu}'} - G_{\text{n}} \sum_{\nu, \nu' > 0} b_{\nu}^{\dagger} b_{\bar{\nu}}^{\dagger} b_{\nu'} b_{\bar{\nu}'}, \quad (3)$$

where G_{p} (G_{n}) is the proton (neutron) average pairing strength. The quadrupole-quadrupole interaction may be expressed as:

$$H_{\text{Q}} = -\frac{1}{2} \sum_{\mu=0,2} \chi^{(\mu)} (:Q_{2\mu}^{\dagger}(p) Q_{2\mu}(p): + :Q_{2\mu}^{\dagger}(n) Q_{2\mu}(n): \\ + 2 :Q_{2\mu}^{\dagger}(p) Q_{2\mu}(n):), \quad (4)$$

with the strength parameter $\chi^{(\mu)}$. The proton quadrupole operator may be expressed as:

$$\begin{aligned}
 Q_{20}^+(p) &= Q_{20}(p) = \sum_{\nu, \nu'} \left\langle \nu \left| r^2 Y_{20} \right| \nu' \right\rangle_p a_{\nu}^+ a_{\nu'}, \\
 Q_{22}^+(p) &= Q_{22}(p) = \sum_{\nu, \nu'} \left\langle \nu \left| \frac{r^2}{\sqrt{2}} (Y_{22} + Y_{2-2}) \right| \nu' \right\rangle_p a_{\nu}^+ a_{\nu'}
 \end{aligned} \quad (5)$$

$Q_{2\mu}^+(n)$ and $Q_{2\mu}(n)$ can be written down similarly.

To obtain the reliable information about the intrinsic structure of each band, H_{intr} can be diagonalized in a sufficiently large many-particle configuration space in which the particle number is conserved (referred as particle-number-conserving, PNC, method[12]*). It should be emphasized that the PNC method is different from the usual shell model calculation in which a single-particle-level truncation is adopted. Instead, in the PNC treatment, a new kind of truncation, the many-particle configuration truncation, is suggested. Theoretically, it is natural to diagonalize Hamiltonian with certain many-body configuration energy truncation because the system treated is a many-body system. Practically, in the usual single-particle-level truncation, on the one hand, a great number of configurations, which are very unimportant for the low-lying excited states of a many-body system, are involved and make the computation very tedious and time consuming; on the other hand, a large number of relatively important configurations are omitted[13]. The configuration space needed in the PNC calculation is not very large as we are interested only in the properties of ground band and low-lying excited bands. Calculation shows that for low-lying excited bands the number of important configurations (weight $\geq 1\%$) is very limited and their energies are not too high. The PNC treatment turns out to be practicable for obtaining a sufficiently accurate solution to the low-lying excited states of a many-particle system, provided the configuration space is not too large. In Ref.[12], only pairing force was considered. A generalization to treat the long range quadrupole-quadrupole force is given in the present paper.

In the PNC treatment, the nuclear configuration is a product of proton configuration and neutron configuration. As an illustration, the expressions for the various proton configurations are given as follows.

(1) The configurations of $K = 0$ are

$$\begin{aligned}
 &|\rho_1 \bar{\rho}_1 \rho_2 \bar{\rho}_2 \cdots \rho_n \bar{\rho}_n\rangle \quad (\pi = +), \\
 &|\mu \nu \rho_1 \bar{\rho}_1 \cdots \rho_{n-1} \bar{\rho}_{n-1}\rangle \quad (\mathcal{Q}_\mu + \mathcal{Q}_\nu = 0, \pi = \pi_\mu \pi_\nu), \\
 &\dots\dots\dots
 \end{aligned} \quad (6)$$

(2) The configurations of $K \neq 0$ are

$$\begin{aligned}
 &|\mu \nu \rho_1 \bar{\rho}_1 \cdots \rho_{n-1} \bar{\rho}_{n-1}\rangle \quad (K = \mathcal{Q}_\mu + \mathcal{Q}_\nu, \pi = \pi_\mu \pi_\nu) \\
 &\dots\dots\dots
 \end{aligned} \quad (7)$$

If only the pairing force is taken into account, the seniority ν is a good quantum number. However, the quadrupole-quadrupole interaction may lead to a coupling between the configurations of different seniorities. Furthermore, due to the n-p interaction, the couplings between proton and

*The method used in this paper is a generalization of Ref.[12] to including a long range quadrupole-quadrupole force. Conventionally the eigenspectra of H_{intr} are obtained with the BCS method (independent quasiparticle approximation) in which a particle-quasiparticle transformation is introduced and H_{intr} is approximately replaced by a sum of independent quasiparticle Hamiltonians. Because of the appearance of a number of spurious states and the difficulty in dealing with the blocking effect, the reliability of the BCS results is ambiguous. In the present paper the PNC method is used. The difficulties encountered in BCS method disappear in the PNC treatment, but the computational work is more time consuming.

neutron configurations will happen. Therefore, the intrinsic Hamiltonian (1) should be diagonalized in a configuration space of the nucleus with fixed $K = K_p + K_n$ and parity (in this paper we will confine ourselves to the case of even parity). The eigenenergies and corresponding wave functions are denoted by $E_{K\alpha}$ and $|K\alpha\rangle$, respectively, where $\alpha = 0$ (the lowest band for a given K), 1, 2, 3, ... (excited bands).

It is well known that the electromagnetic transition probability depends more sensitively on the intrinsic wave function than the energy does. Therefore, we may test the reliability of various nuclear models more effectively by comparing the calculated transition probabilities with the experiments. In this paper, we are mainly concentrated on the $E2$ transition, because abundance of $B(E2)$ data are available. The reduced $E2$ transition probability is expressed as[14]:

$$B(E2; I_i K_i \rightarrow I_f K_f) = |\langle I_i K_i 2 K_f - K_i | I_f K_f \rangle|^2 \cdot |\langle K_f \alpha_f | M'(2, K_f - K_i) | K_i \alpha_i \rangle|^2 \cdot (1 + \delta_{K_i K_f, 0}) \quad (8)$$

where i and f denote the initial and the final states, respectively, and

$$M'(2, \mu) = \sum_{\nu, \nu'} e_{\text{eff}}^p \langle \nu | r^2 Y_{2\mu} | \nu' \rangle a_{\nu}^+ a_{\nu'} + \sum_{\lambda, \lambda'} e_{\text{eff}}^n \langle \lambda | r^2 Y_{2\mu} | \lambda' \rangle b_{\lambda}^+ b_{\lambda'}, \quad (9)$$

is the electric quadrupole transition operator expressed in the rotating frame, e_{eff}^p and e_{eff}^n are the effective charges of proton and neutron, respectively[15].

3. RESULTS AND DISCUSSIONS

3.1 Choice of the Parameter Values

As mentioned above, the values of the Nilsson Parameters are taken from Ref.[10] and the Lund systematics[11]. For ^{168}Er , they are as follows:

quadrupole deformation δ_2	hexadecupole deformation δ_4	μ		κ	
		neutron	proton	neutron	proton
0.272	0.022	0.4167	0.602	0.0631	0.0630

In the present calculation, the truncated configuration energy is taken as $E_c = 0.6\hbar\omega_{00}$ (so that all the important configurations in the ground band and the low-lying bands are included in the calculation), $\hbar\omega_{00} = 41A^{-1/3}$ MeV = 7.43 MeV. The parameters G_p and G_n can be determined by fitting the observed odd-even mass difference taken from the Atomic Mass Table (1985)[16]. In practical calculation, however, it is found that the results will be more consistent with the experiments if G is decreased by about 10%. This reduction also appears in the BCS treatment for the rare-earth nuclei, i.e., the energy gap parameter should multiply by an attenuation factor[17]. In case $E_c = 0.6\hbar\omega_{00}$, the pairing strength parameters are:

$$G_p/\hbar\omega_{(1)} = 0.0414; \quad G_n/\hbar\omega_{(1)} = 0.0343. \quad (10)$$

The parameters of quadrupole force strength are:

$$\chi^{(0)} = 0.008 \left(\frac{M\omega_0}{\hbar} \right)^2 \hbar\omega_{00}; \quad \chi^{(2)} = 0.08 \left(\frac{M\omega_0}{\hbar} \right)^2 \hbar\omega_{00}, \quad (11)$$

where

$$\omega_0 = \omega_{00} \left[\left(1 + \frac{2}{3} \varepsilon_2 \right)^2 \left(1 - \frac{4}{3} \varepsilon_2 \right) \right]^{-1/3}. \quad (12)$$

The effective charges e_{eff}^p and e_{eff}^n are determined by the observed $B(E2; 2, 0_1^+ \rightarrow 0, 0_1^+)$ and $B(E2; 2, 2_1^+ \rightarrow 2, 0_1^+)$ values in ^{168}Er [18],

$$e_{eff}^p = 1.65e; \quad e_{eff}^n = 1.58e. \quad (13)$$

Once the above parameters are chosen, the wave functions and energy spectra of the low-lying excited states can be calculated, hence the related $E2$ transition probabilities can be derived. The results are given in Figs.1--4 and Tables 1--6.

TABLE 1
Several Important B(E2) Branching Ratios of 0_2^+ Band

branching ratios	Exp	IBM	this paper
$\frac{0_2^+}{K=0_2^+} \rightarrow \frac{2_2^+}{K=0_2^+}$ $\frac{0_2^+}{K=0_2^+} \rightarrow \frac{2_2^+}{K=2_2^+}$	≥ 0.196	0.055	0.195
$\frac{4_2^+}{K=0_2^+} \rightarrow \frac{2_2^+}{K=0_2^+}$ $\frac{4_2^+}{K=0_2^+} \rightarrow \frac{2_2^+}{K=2_2^+}$	0.0002	0.0009	0.00028
$\frac{2_2^+}{K=0_2^+} \rightarrow \frac{0_2^+}{K=0_2^+}$ $\frac{2_2^+}{K=0_2^+} \rightarrow \frac{3_2^+}{K=2_2^+}$	0.047	0.020	0.110

*Except 0_4^+ band, all the experimental values and IBM calculation results in the tables are taken from Ref.[6].

TABLE 2
Several Important $B(E2)$ Branching Ratios of 0_3^+ Band

branching ratios	Exp	IBM	this paper
$\frac{0_3^+ \xrightarrow{K=0_3^+} 2_3^+}{0_3^+ \xrightarrow{K=0_3^+} 2_1^+}$	<1.8	232.5	1.23
$\frac{4_3^+ \xrightarrow{K=0_3^+} 2_3^+}{4_3^+ \xrightarrow{K=0_3^+} 2_1^+}$	0.0008	0.0004	0.0002
$\frac{6_3^+ \xrightarrow{K=0_3^+} 4_3^+}{6_3^+ \xrightarrow{K=0_3^+} 4_1^+}$	0.0048	0.00006	0.0036

TABLE 3
Comparison of Experimental and Calculated $B(E2)$
Branching Ratios from the 0_2 Band in ^{168}Er

transitions		relative $B(E2; I_i \rightarrow I_f)$		
I_i^π	I_f^π, K	Exp	IBM	this paper
0+	2+, 0	$\equiv 5.5^{1)}$	5.5	5.5
	2+, 2	<28.0	100.0	28.2
2+	0+, 0	0.23	0.10	0.54
	4+, 0	1.4	0.32	1.0
	2+, 2	4.0	2.6	2.8
	3+, 2	$\equiv 4.9$	4.9	4.9
	0+, 0' ²⁾		100.0	1350.0
4+	2+, 0	0.02	0.09	0.028
	6+, 0	0.11	0.23	0.04
	2+, 2	0.03	0.04	0.004
	3+, 2	0.35	0.63	0.06
	4+, 2	0.52	2.2	0.17
	5+, 2	0.19	2.8	0.19
	2+, 0'	100.0	100.0	100.0
6+	4+, 0	0.02	0.07	0.028
	8+, 0	0.07	0.21	0.033
	4+, 2	0.11	0.09	0.01
	5+, 2	0.32	0.73	0.07
	6+, 2	0.93	2.0	0.17
	4+, 0'	100.0	100.0	100.0

1) The notation " \equiv " defines the transitions used for normalization in case an intraband transition was not observed. This notation is also used in Table 4.

2) The notation 0' refers to the 0_2^+ band.

3.2 Energy Spectrum

As seen from Figs.1-3, in comparison of the IBM prediction, the agreement between the calculated $K^\pi = 0^+, 2^+, 3^+$ and the experimental results is much improved.

(a) $K^\pi = 0^+$ bands. There have been observed three 0^+ excited bands. The calculated counterparts by using the PNC method are close to them. The main configurations of each 0^+ band are listed in the caption below Fig.1.

TABLE 4
Comparison of Experimental and Calculated $B(E2)$
Branching Ratios from the 0_3^+ Band in ^{168}Er

transitions		relative $B(E2; I_i \rightarrow I_f)$		
I_i^π	I_f^π, K	Exp	IBM	this paper
0^+	$2^+, 0$	$\cong 0.43$	0.43	0.43
	$2^+, 2$	< 0.8	100.0	0.53
	$2^+, 0'$	< 59.0	0.46	0.013
2^+	$0^+, 0$	0.09	0.006	1.5
	$4^+, 0$	1.0	0.02	3.8
	$2^+, 2$	1.4	2.3	1.8
	$3^+, 2$	2.0	4.3	4.6
	$4^+, 2$	$\cong 2.0$	2.0	2.0
	$0^+, 0'$	< 7.0	0.004	0.04
	$2^+, 0'$	< 7.0	0.01	0.06
	$4^+, 0'$	< 3000.0	0.03	0.10
	$0^+, 0''$	< 4000.0	100.0	336.6
4^+	$2^+, 0$	0.01	0.005	0.49
	$6^+, 0$	0.34	0.01	0.78
	$2^+, 2$	0.08	0.04	0.02
	$3^+, 2$	0.08	0.58	0.24
	$5^+, 2$	0.48	2.4	0.83
	$6^+, 2$	< 0.4	1.1	0.3
	$2^+, 0'$	< 4.0	0.002	0.015
	$4^+, 0'$	< 3.0	0.01	0.014
	$2^+, 0''$	100.0	100.0	100.0
6^+	$4^+, 0$	0.05	0.004	0.45
	$6^+, 0$	0.48	0.006	0.36
	$8^+, 0$	0.32	0.01	0.61
	$5^+, 2$	< 0.3	0.69	0.27
	$6^+, 2$	< 40.0	1.7	0.64
	$7^+, 2$	< 0.6	2.0	0.60
	$8^+, 2$	< 6.0	0.90	0.20
	$4^+, 0'$	< 0.6	0.001	0.014
	$6^+, 0'$	< 6.0	0.03	0.011
	$4^+, 0''$	100.0	100.0	100.0

TABLE 5
Comparison of Experimental and Calculated $B(E2)$
Branching Ratios from the 0_1^+ Band in $^{168}\text{Er}^*$

transitions		relative $B(E2; I_i \rightarrow I_f)$	
I_i^+	I_f^+, K	Exp	this paper
2^+	$2^+, 2$	18.0	8.0
	$3^+, 2$	54.0	20.0
	$0^+, 0'$	100.0	100.0
4^+	$3^+, 2$	37.0	32.0
	$4^+, 2$	100.0	100.0
6^+	$6^+, 2$	105.0	20.0
	$7^+, 2$	100.0	100.0

*The experimental data are taken from Ref.[3].

TABLE 6
Comparison of Experimental and Calculated $B(E2)$
Branching Ratios from the γ Band in ^{168}Er

transitions		relative $B(E2; I_i \rightarrow I_f)$		
I_i^+	I_f^+, K	Exp	IBM	this paper
2^+	$0^+, 0$	54.0	66.0	70.0
	$2^+, 0$	100.0	100.0	100.0
	$4^+, 0$	6.8	6.0	5.0
3^+	$2^+, 0$	2.6	2.7	4.5
	$4^+, 0$	1.7	1.3	1.8
	$2^+, 2$	100.0	100.0	100.0
4^+	$2^+, 0$	1.6	2.5	4.5
	$4^+, 0$	8.1	8.3	13.4
	$6^+, 0$	1.1	1.0	1.1
5^+	$2^+, 2$	100.0	100.0	100.0
	$4^+, 0$	2.9	4.3	7.5
	$6^+, 0$	3.6	3.1	4.3
6^+	$3^+, 2$	100.0	100.0	100.0
	$4^+, 2$	122.0	98.0	100.0
	$4^+, 0$	0.44	0.97	1.8
7^+	$6^+, 0$	3.8	4.3	7.0
	$8^+, 0$	1.4	0.73	0.75
	$4^+, 2$	100.0	100.0	100.0
8^+	$5^+, 2$	69.0	59.0	60.0
	$6^+, 0$	0.74	2.7	5.2
	$5^+, 2$	100.0	100.0	100.0
9^+	$6^+, 2$	59.0	39.0	93.0
	$6^+, 0$	1.8	0.67	1.4
	$7^+, 0$	5.1	3.5	5.9
10^+	$6^+, 2$	100.0	100.0	100.0
	$7^+, 2$	135.0	29.0	36.0

(b) $K^\pi = 2^+$ bands. Apart from the lowest $K^\pi = 2^+$ band (γ -band), four low-lying $K^\pi = 2^+$ bands were observed at about 2 MeV. The pattern of the calculated low-lying $K^\pi = 2^+$ bands is similar to

the observed results. The lowest 2_1^+ band (γ -band) shows a strong collectivity; 2_2^+ band is a two-pair-broken band (4-quasiparticle excitation); 2_3^+ band is a rather pure pair-broken band (2-quasiparticle excitation); but 2_4^+ and 2_5^+ bands are not so pure. In comparison with the IBM calculation, which predicted a 2_3^+ band at too high energy, obvious improvement is obtained in the PNC calculation.

(c) $K^\pi = 3^+$ bands. The calculated two lowest 3^+ bands by using the PNC method are very close to the observed 3^+ bands, which show a rather pure pair-broken character, hence are of weak collectivity. In the IBM description, the 3^+ bands may be expected only if the g bosons are included. In the calculation of the low-lying spectra of ^{168}Er in the frame of sdg -IBM by Arima et.al.[8], and by H. C. Wu and X. Q. Zhou[22], indeed a 3^+ band was reproduced. However, in their calculation appear more bands which have not been observed in the experiment.

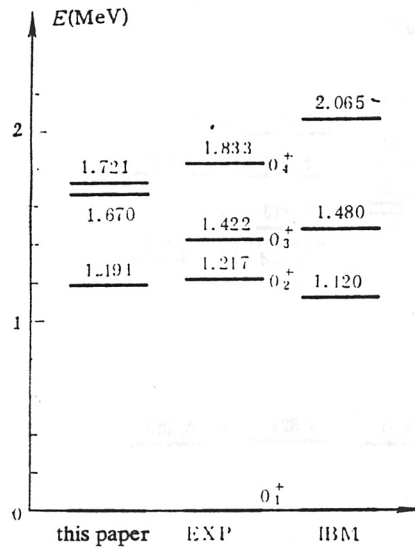


FIG.1 The positions of the $K^\pi = 0^+$ band heads. The experimental values in all the figures are taken from Refs. [2] and [7]. For convenience, the ground configuration is denoted by $|0\rangle$, while $|633\uparrow \rightarrow 521\downarrow\rangle$ indicates the state that one pair of particles in the ground configuration excites from $633\uparrow$ state to $521\downarrow$ state, the others are on the analogy of this. The calculated important configuration components of the $K^\pi = 0^+$ band are as follows:

	$ 0\rangle$	$n 633\uparrow \rightarrow 521\downarrow\rangle$	$n 505\uparrow \rightarrow 521\downarrow\rangle$	$p 523\uparrow \rightarrow 541\downarrow\rangle$
0_1^+	0.61	0.09	0.07	0.05
0_2^+	0.11	0.26	0.31	0.22
0_3^+	0.14			0.58
0_4^+		0.47	0.30	0.07

(d) $K^\pi = 4^+$ bands. Similar to the sd -IBM results, the present calculation also predicts a $K^\pi = 4^+$ band at about 1600 keV, which is lower than the observed value. It is found that the 4^+ band is mainly a proton pair-broken band $p\{[523]_{\frac{7}{2}}^- + [541]_{\frac{1}{2}}^-\}$. The position of this band in the calculation is very sensitive to the single particle level scheme. Especially, it is strongly influenced by the

quadrupole force because the Y_{20} diagonal matrix element in the state $p[541]_{\frac{1}{2}}^{-}$ is very large. Therefore, the position of this excited band will be affected even by a slight change of the quadrupole force strength or the single particle state. It is well known that the present Nilsson level scheme (in the Lund systematics) is good for describing the single neutron levels of rare-earth nuclei, but not so satisfactory for the single proton levels. If a more realistic single particle wave function (such as, those obtained in a Woods-Saxon potential) is adopted, the results would be improved. Besides, the main configuration of $K^{\pi} = 4_1^{+}$ band is $p\{[523\uparrow]_{\frac{1}{2}}^{-} + [541\downarrow]_{\frac{1}{2}}^{-}\}$, while that of $K^{\pi} = 3_1^{+}$ band is $p\{[523\uparrow]_{\frac{1}{2}}^{-} [541\downarrow]_{\frac{1}{2}}^{-}\}$. Their bandheads coincide if no other residual interactions are considered. However, if a spin-spin interaction is taken into account, the position of 4_1^{+} bandhead will rise higher according to the Gallagher rule[19], and makes the calculated result closer to the observed one.

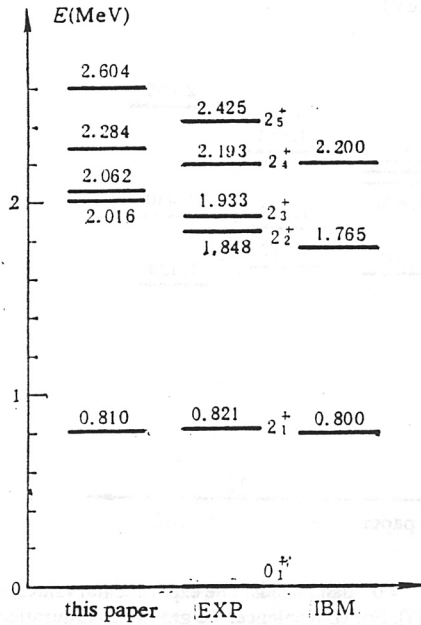


FIG.2 The positions of the $K^{\pi} = 2^{+}$ band heads. The calculated important configuration components of the $K^{\pi} = 2^{+}$ band are as follows:

	$n(521\uparrow + 521\downarrow)$	$n(523\downarrow - 521\downarrow)$	$p(413\downarrow - 411\downarrow)$	$p(411\uparrow + 411\downarrow)$	$n(505\uparrow + 521\downarrow)$ $p(523\uparrow + 541\downarrow)$
2_1^{+}	0.12	0.33	0.17	0.33	1.0
2_2^{+}					
2_3^{+}		0.92			
2_4^{+}		0.32	0.12	0.48	
2_5^{+}	0.32	0.27	0.24	0.10	

3.3 E2 Transition Probability

The calculated $B(E2)$ branching ratio and comparison with experiments are shown in Tables 1 through 6. But only a few transitions of the 0^{+} excited bands are discussed as below.

(a) $E2$ transitions from 0_2^+ band (β -band). Some important results are shown in Table 1 and the detailed results are given in Table 3. Experimentally the de-excitation of 0_2^+ band is mainly through the $E2$ transition to 2_1^+ band (γ -band) while the decay to the ground band is relatively weak. This phenomenon is well reproduced both in the PNC and the IBM calculations. In the PNC treatment, this result is governed by the intrinsic structure of 0_2^+ band and 2_1^+ band. Similar behavior was observed also in nuclei ^{150}Gd and ^{172}Yb [20,21] and may be regarded as a rather general feature in well-deformed even-even rare-earth nuclei. The present calculation shows that this phenomenon may be well accounted for by the microscopic theory of pairing plus the quadrupole-quadrupole force model.

(b) $E2$ transitions from the 0_3^+ band. The results of the $B(E2)$ calculations for transitions from the 0_3^+ band are given in Table 4 and some important results are shown in Table 2. $B(E2)$ values concerning the 0_3^+ band have not been observed so precisely as those of the 0_2^+ band. However, the observed $E2$ transitions from the 0_3^+ band to the ground band are basically accurate. The calculated values for these transitions by using the PNC method are of the same order of magnitude as the observed results, while the predictions by the sd -IBM are two orders of magnitude smaller than the observed results.

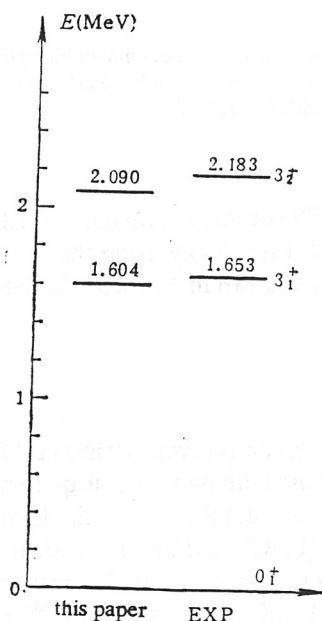


FIG.3 The positions of the $K^\pi = 3^+$ band heads. The calculated important configuration components of the $K^\pi = 3^+$ band are as follows: 3_1^+ band: $p(523\uparrow - 541\downarrow)$ 1.00; 3_2^+ band: $n(523\downarrow + 521\downarrow)$ 0.98.

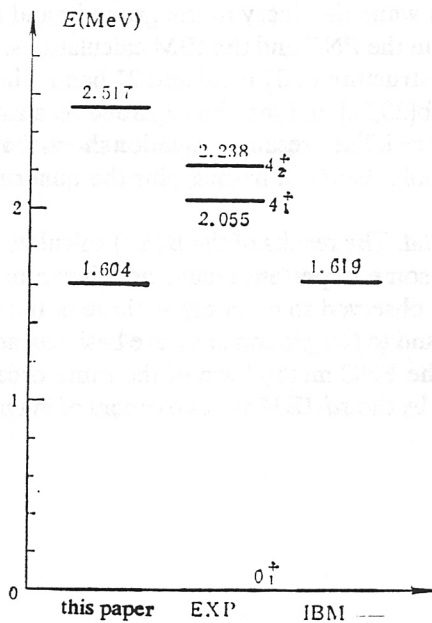


FIG.4 The positions of the $K^\pi = 4^+$ band heads. The calculated important configuration components of the $K^\pi = 4^+$ band are as follows: 4^+ band: $p(523\uparrow + 541\downarrow)$ 1.00; 4^+ band: $n(505\uparrow + 521\downarrow)p(411\downarrow - 413\downarrow)$ 0.57; $n(505\uparrow - 521\uparrow)$ 0.38.

(c) $E2$ transitions from the 0_4^+ band. The experimental data of $E2$ transitions concerning the 0_4^+ band are taken from Ref.[3]. The calculated results by using the PNC method agree well with the experiments. Detailed calculated results are shown in Table 5. No IBM prediction has been seen in the literature.

4. CONCLUSION

The intrinsic properties of the low-lying bands (even-parity) in ^{168}Er were analyzed in the frame of the Bohr-Mottelson-Nilsson model in which the pairing plus quadrupole-quadrupole interaction has been taken into account. In order to obtain detailed and reliable information about the intrinsic structure, the particle-number-conserving (PNC) method was used, in which the blocking effects are taken into account exactly. This treatment turns out to be rather successful for a consistent description of the energy levels and the related $E2$ transitions in ^{168}Er .

ACKNOWLEDGEMENT

The authors are grateful to Professors Zhang Xizhen and Cheng Tansheng for their valuable discussions and suggestions.

REFERENCES

- [1] W. F. Davidson, D. D. Warner, R. F. Casten, et al., J. Phys. G7(1981)455; G7(1981)843.
- [2] W. F. Davidson, W. R. Dixon and R. S. Stony, Can. J. Phys. 62(1984)1538.

- [3] W. F. Davidson, W. R. Dixon, D. G. Burke and J. A. Cizewski, *Phys. Lett.* **130B**(1983)160.
- [4] D. G. Burke, B. L. W. Maddock and W. F. Davidson, *Nucl. Phys.* **A442**(1985)424.
- [5] D. G. Burke, W. F. Davidson, J. A. Cizewski, R. E. Brown and J. W. Sunier, *Nucl. Phys.* **A445**(1985)70.
- [6] D. D. Warner, R. F. Casten and W. F. Davidson, *Phys. Rev.* **C24**(1981)1713.
- [7] A. Bohr and B. R. Mottelson, *Phys. Scr.* **25**(1982)28.
- [8] N. Yoshinaga, Y. Akiyama and A. Arima, *Phys. Rev. Lett.* **56**(1986)1116.
- [9] D. R. Bes and R. A. Sorensen, *Adv. Nucl. Phys.* **2**(1969)129.
- [10] S. G. Nilsson, et al., *Nucl. Phys.* **A131**(1969)1.
- [11] R. Bengtsson, *J. de Phys.* **41**(1980)C10--84.
- [12] J. Y. Zeng and T. S. Cheng, *Nucl. Phys.* **A405**(1983)1.
- [13] J. Y. Zeng, T. S. Cheng, L. Cheng and C. S. Wu, *Nucl. Phys.* **A421**(1984)125c.
- [14] A. Bohr and B. R. Mottelson, *Nuclear Structure*, Vol. II,
- [15] R. D. Lawson, *Theory of the Nuclear Shell Model*.
- [16] A. H. Wapstra and G. Audi, *Nucl. Phys.* **A432**(1985)40.
- [17] S. G. Nilsson and O. Prior, *Mat. Fys. Medd. Dan. Vid. Selsk.* **32**(1961), No. 16.
- [18] L. M. Greenwood, *Nucl. Data Sheets*, **11**(1974)385.
- [19] C. J. Gallagher, Jr., *Phys. Rev.* **126**(1962)1525.
- [20] R. C. Greenwood, et al., *Nucl. Phys.*, **A304**(1978)327.
- [21] C. W. Reich, R. C. Greenwood and R. A. Lokken, *Nucl. Phys.*, **A228**(1974)365.
- [22] H. C. Wu and X. Q. Zhou, *Nucl. Phys.*, **A417**(1984)67.